AN EXPERIMENTAL STUDY ON ENTROPY GENERATION IN THE FATIGUE OF FIBER-REINFORCED THERMOPLASTIC COMPOSITES

Pessoa, S.[1], Marques, R.[2], Ali, H. Q.[3,4,5] , Yildiz, M.[3,4,5] and Suleman, A.[1,2]*
[1]IDMEC, Instituto Superior Técnico, Universidade de Lisboa, Lisbon, Portugal
[2] Department of Mechanical Engineering, University of Victoria, Victoria, BC, Canada
[3] Integrated Manufacturing Technologies Research and Application Center, Sabanci University, Istanbul, Turkey
[4] Composite Technologies Center of Excellence, Sabanci University-Kordsa, Istanbul, Turkey
[5] Faculty of Engineering and Natural Sciences, Materials Science and Nano Engineering, Sabanci University, Istanbul, Turkey
* Corresponding author (suleman@uvic.ca)

Keywords: *structural health monitoring, fatigue life prediction, entropy generation*

ABSTRACT

Fracture fatigue entropy (FFE) has proven to be independent of the loading condition or stacking sequence, thus emerging as a promising fatigue failure criterion for metals and composites. However, existing works are limited to materials with rate-independent behavior and to the best of the authors' knowledge, the formulation of FFE has not yet been successfully extended to thermoplastic composites. The present work delivers a preliminary study on the effects of stress and frequency in the accumulated generated entropy due to plastic deformation and heat flux by conduction during fatigue using the Clausius-Duhem inequality. Fatigue tests were conducted on carbon fiber/PEKK dog-bone specimens with angle-ply and quasi-isotropic configurations at four test conditions comprising two stress levels and two loading frequencies. Full-field temperature measurements were obtained using an infrared thermal camera, while full-field in-plane strains were measured with a "low-cost" digital image correlation system. The accumulated entropy at the time of failure proved to be a function of the fatigue life, thus highlighting the need to consider the influence of viscous, damage, and hardening dissipative terms on the total accumulated entropy.

1 INTRODUCTION

For the past decades, industries like aerospace have been employing almost exclusively composites with thermoset matrices due to the well-established knowledge and certified processes available. Nevertheless, the incorporation of thermoplastic composites is becoming more common as they present advantages such as high impact toughness, higher damage tolerance, low moisture absorption, unlimited shelf life at ambient temperature, faster production cycles, and the ability to be recycled [1].
Since fatigue is one of the most critical phenomena affecting the structural integrity of components in engineering, a proper understanding of fatigue behavior is of the utmost importance. However, predicting the fatigue life of composites is a difficult task due to their heterogeneity, anisotropy, and presence of multiple damage modes. Several approaches for fatigue life prediction have been proposed, namely stress-life and energy-based methods. Yet, these methods are sensitive to the loading conditions and show a large scatter of data. The efforts to have a more unified fatigue failure criterion culminated in entropy-based approaches, as proposed by Naderi et al. [2]. The premise of their work is that fatigue damage accumulation is accompanied by irreversible energy dissipation, and such process generates entropy in accordance with the second law of thermodynamics. Also, the concept of fracture fatigue entropy (FFE) is introduced as the cumulative entropy production up to the fracture point, and it was

assumed as independent of loading amplitude, frequency, and geometry [3-5]. Most studies have been performed on metallic materials and a few on thermoset-based composites, but to the best of the authors' knowledge, this concept has not been applied to thermoplastics, whose effects of viscosity, temperature, and damage must be simultaneously considered. Moreover, entropy calculations performed in most studies disregarded the contribution of some dissipative terms under the assumption of having negligible orders of magnitude for such materials. In this work, a similar approach to FFE is taken by calculating the same dissipative terms for tests at different loads, frequencies, and stacking sequences. On the other hand, a more comprehensive theoretical formulation is derived for further improvement of the generated entropy measurements.

2 THEORETICAL BACKGROUND

2.1 Thermodynamic laws

In the more general case of large deformations (or finite strains), body motion can be described from different standpoints depending on the configuration where position and time are being framed. Given that the initial geometry of the material is well known, all physical measures present in the following thermodynamic and constitutive laws will be represented with respect to an *undeformed* configuration. Using the localization theorem and a multiplicative decomposition of the deformation gradient, F , the balance of thermal energy can be expressed in the *undeformed* configuration as,

$$\rho_0 \dot{u} = \left[F^{-1} P \cdot \left(\dot{E_{ve}} + \dot{E_{vp}}\right) + \rho_0\, \dot{w_f}\right] - \nabla \cdot q_0, \tag{1}$$

where ρ_0 is the density in the undamaged configuration, u is the internal energy per unit mass, P is the first Piola-Kirchoff stress tensor, w_f is the generated energy per unit mass due to dissipative phenomena (damage formation, friction), $\dot{E_{ve}}$ and $\dot{E_{vp}}$ are the Lagrangian viscoelastic and viscoplastic strain rate tensors, respectively, and q_0 is the heat flux transferred by conduction, convection, and radiation. The term inside squared brackets corresponds to the hysteresis energy per unit volume, h .

Based on the Clausius statement, the local form of the second law of thermodynamics can be written as,

$$\dot{\gamma}\theta \;=\; F^{-1} P \cdot \left(\dot{E_{ve}} + \dot{E_{vp}}\right) - \rho_0\left(\dot{\psi} + \dot{\theta}\eta\right) - q_k \cdot \frac{\nabla\theta}{\theta} \geq 0, \tag{2}$$

Where η and γ represent entropy per unit mass and unit volume, respectively, ψ is the Helmholtz free energy per unit mass, q_k is the heat flux due to conduction only, and θ is the absolute temperature. In this work, the entropy of interest is γ that will be non-zero under the presence of dissipative phenomena. The thermodynamic law of equation (2) imposes a natural condition to the mathematical description of the material's constitutive law.

2.2 Constitutive law and entropy generation

The Helmholtz free energy of the thermoplastic composite under study is assumed to be split into viscoelastic and viscoplastic components, $\psi = \psi_{ve} + \psi_{vp}$. According to the thermodynamic theory for materials with memory, each component must be a function of the current and past histories of the variables in their respective arguments. Therefore, ψ_{ve} is assumed to be a functional of the viscoelastic Lagrangian strain (E_{ve}), the absolute temperature θ, and a scalar damage variable, D ,

$$\psi_{ve}(t) = \int_0^\infty \psi\{E_{ve}(t-s), \theta(t-s), D(t-s)\} ds. \tag{3}$$

The viscoplastic component of the Helmholtz free energy is assumed to depend on the history of θ, and isotropic and kinematic hardening scalar variables, r and α respectively,

$$\psi_{vp}(t) = \int_0^\infty \psi\{\theta(t-s), \alpha(t-s), r(t-s)\} ds. \tag{4}$$

The final form of the dissipation inequality can be obtained from integrating the following terms between each full loading cycle,

$$\int_0^T \dot{\gamma}\theta \; dt = \int_0^T \left[F^{-1}P \cdot \dot{E_{vp}} - q_k \cdot \frac{\nabla\theta}{\theta} - \rho\left(\dot{\eta_v} + \frac{\partial\psi_{vp}}{\partial V} \cdot \dot{V}(t) + \frac{\partial\psi_{ve}}{\partial D}\dot{D}(t)\right)\right] dt \geq 0, \qquad (5)$$

where T is the period of a loading cycle, η_v is the entropy per unit mass generated due to viscous phenomena, and V is a vector containing both isotropic and kinematic hardening variables. In the present paper, focus will be given to the calculation of the first two terms on the RHS of equation (5).

3 MATERIAL AND EXPERIMENTAL PROCEDURE

The composite used in this study is a carbon fiber reinforced polyetherketoneketone (PEKK). Prepreg tapes of Toray TC1320 were laid up into sixteen-ply plates using automated fiber placement and subjected to post-consolidation in the autoclave. Two stacking sequences were considered: angle-ply (AP) [+45/-45]4s and quasi-isotropic (QI) [0/+45/-45/90]2s. The selection of these two stacking sequences is justified by the research interest underlying the temperature- and rate-dependent behavior of the thermoplastic matrix in the AP configuration and the high applicability of the QI configuration in aircraft components.

Specimens were cut from the plates using water-jet machining. Regarding the geometry of the specimens, it has been reported that the rectangular shape proposed by the ASTM D3479/D3479M standard test method for tension-tension fatigue of PMCs might not be adequate for high frequencies, failing within the gripping area [10]. To overcome this issue, the dog-bone geometry shown in Figure 1 was proposed.

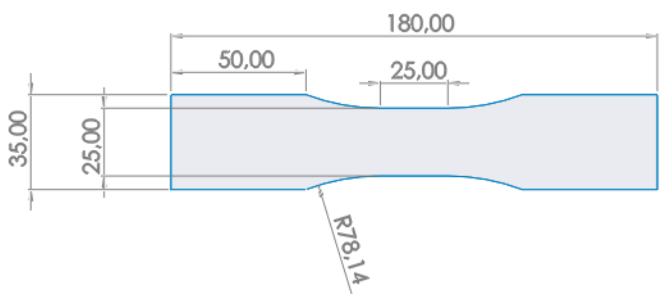

Figure 1. Specimen for fatigue testing (dimensions in millimeters).

Tensile tests to determine the material's ultimate tensile strength (UTS) were conducted at room temperature and strain rates as per the ASTM D3039. The geometry and properties at failure for each stacking sequence are shown in Table 1.

Table 1. Tensile properties of the laminates.

	Width (mm)	Thickness (mm)	Maximum Load (kN)	Ultimate Strength (MPa)	Failure Strain (%)
AP	24.99	2.36	25.33	428.98	22.81
QI	25.04	2.40	37.90	630.75	1.30

Other important thermal-mechanical properties such as the composite's thermal conductivity along the fiber direction and speckle pattern's emissivity were measured and are summarized in Table 2.

Table 2. Material properties

Thermal conductivity (W/mK)	2.6608
Emissivity	0.83

Fatigue tests in load-control mode with a load ratio R=0.1 were conducted using an Instron 8803 servo-hydraulic machine. To study the effect of frequency and stress level on the entropy generation, each stacking sequence was tested at four loading conditions by combining two frequencies (2Hz and 10Hz) and two stress levels (70% and 80% of the UTS for the AP, and 85% and 95% for the QI).

The full-field surface temperature was captured using an infrared camera FLIR X6580sc, whereas the full-field strain field was measured with digital image correlation (DIC). However, traditional DIC cameras available were not sufficient for capturing strain data at the highest frequency, prompting the development of a new system. A digital single-lens reflex (DSLR) camera was chosen to record the fatigue test due to the high video recording frame rate and its low cost when compared to scientific-graded cameras. The parameters related to hardware and strain computation with DIC are stated in Table 3. A schematic of the developed procedure is illustrated in Figure 2.

Table 3. DIC parameters

Camera type	Nikon D3400
Lens	50mm f/1.8
Image size (px × px)	1920x1080
Video frame rate (Hz)	59.94
Aperture	1.8
Software	GOM Correlate
Facet size (px)	22
Point distance (px)	19

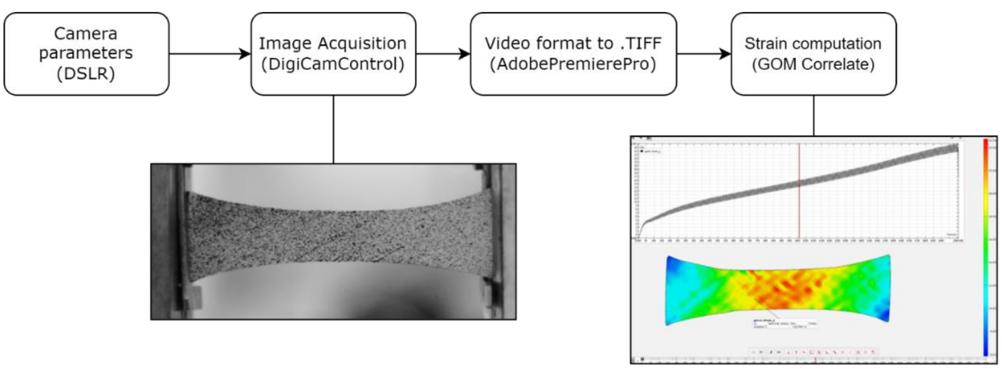

Figure 2. Experimental procedure for “low-cost” DIC

4 RESULTS

4.1 Angle-ply

The formulation of thermodynamic laws (1) and (2) for entropy generation measurements in the AP configuration using a finite strain approach was first validated. Figure 3 shows the time evolution of the Green-Lagrange strain and its linearized version measured with DIC during one of the fatigue tests with AP. The difference observed translates into an error that builds up to more than 10% at the time of failure, which justifies the consideration of finite strain theory for this stacking sequence.

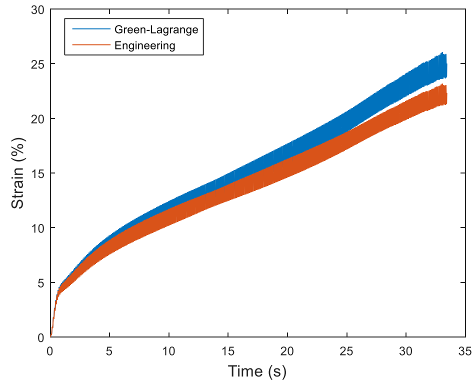

Figure 3. Time evolution of two strain formulations.

4.1.1 Hysteresis Curves

The cyclic stress-strain behavior in fatigue is represented by the hysteresis loops. They consist of loading and unloading paths for each cycle, which do not overlap when viscoelasticity and plasticity occur. This deviation from ideal linear elasticity leads to energy losses in the material that can be quantified by the area enclosed within the loops. The hysteresis curves for the four loading conditions are shown in Figure 4(a)-(d).

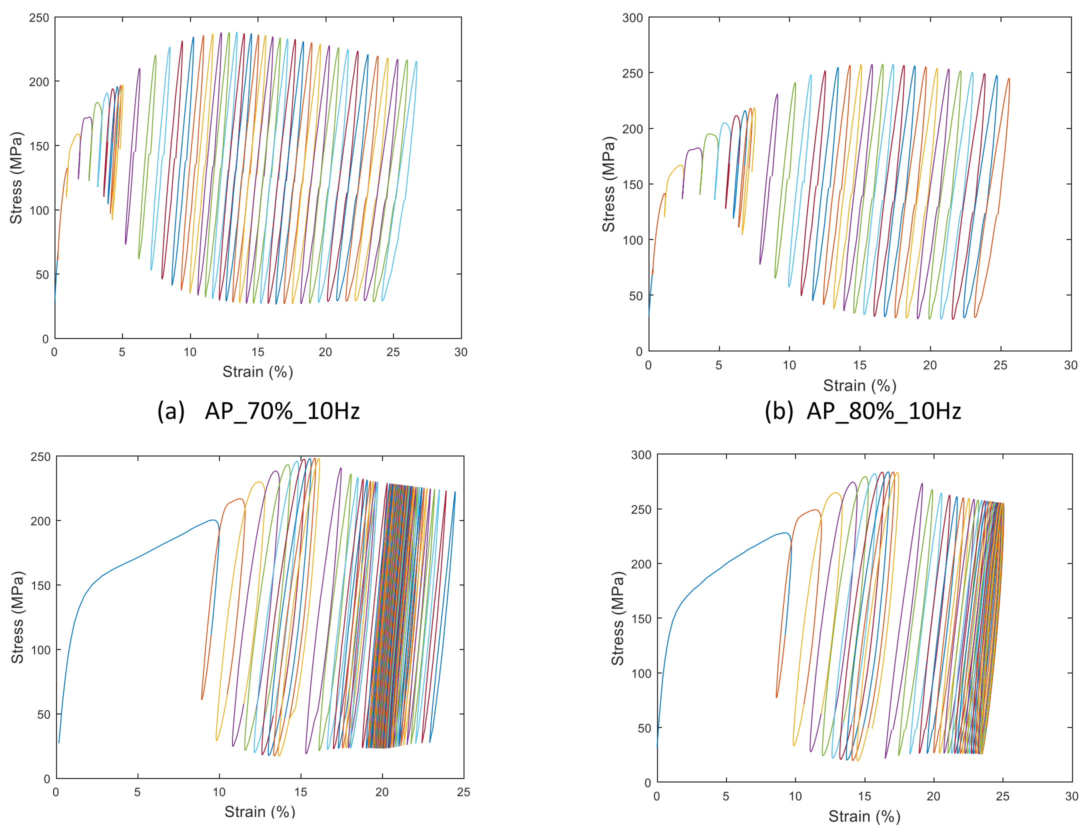

(a) AP_70%_10Hz (b) AP_80%_10Hz

(c) AP_70%_2Hz (d) AP_80%_2Hz

Figure 4. Hysteresis loops.

It is noticeable that tests run at the same frequency yield a similar overall evolution of the loops' area, and differ from the ones at another frequency, with higher dissipated energy in the early stages of the fatigue life for the lower frequency test cases. This observation is justified by the rate-dependent behavior of the PEKK since there is more time for the material to undergo greater deformations under the same applied stress level. For the higher frequency case, the strain response to the applied stress is more instantaneous, which resembles that of an elastoplastic material. In addition, most permanent deformation occurs in the first ten cycles of each test as evidenced by the difference in strain between the start and end points of the loops. During this period, as the peak applied stress gradually approaches the target value, the yield point is still increasing due to the work hardening of the polymer, thus leading to significant plastic deformation.

4.1.2 Entropy due to plastic work

As a first approximation, the plastic work term in the RHS of equation (5) will be assumed equal to the hysteresis energy. The evolution of the respective hysteresis-induced entropy with the normalized life of the material is plotted in Figure 5.

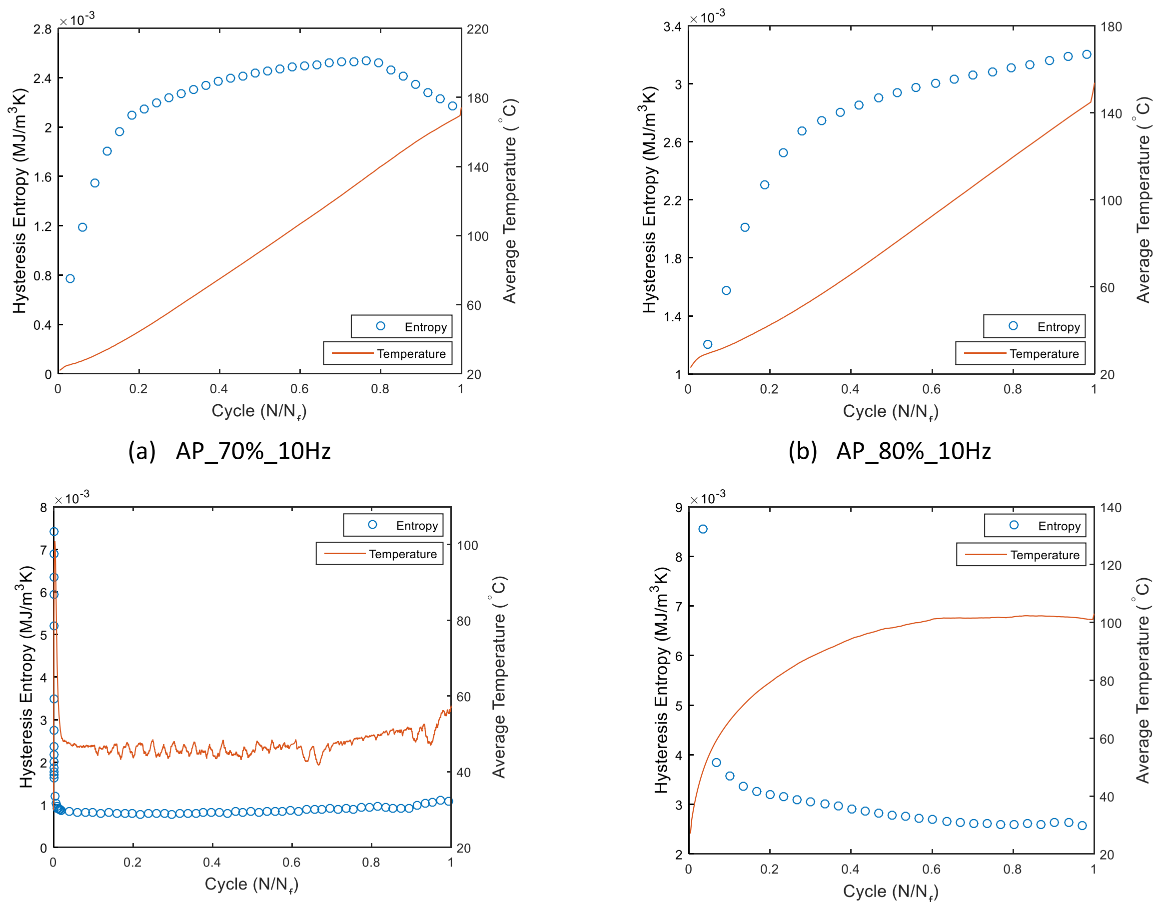

(a) AP_70%_10Hz (b) AP_80%_10Hz

(c) AP_70%_2Hz (d) AP_80%_2Hz

Figure 5. Entropy evolution.

Similar trends of entropy evolution can be observed for tests conducted at the same loading frequency, in accordance with the findings reported in section 4.1.1. An increase in entropy generation followed by a linear rise in average temperature to near the glass transition temperature (T_g = 160°C) for the 10Hz cases can be observed in

Figures 5(a) and (b). The high loading frequency combined with the low thermal conductivity of the matrix material prevents energy due to irreversible phenomena from dissipating to the environment, thus leading to adiabatic heating. The subsequent increase in temperature is stored in the system as internal energy that can be measured in the hysteresis loops as per equation (1). On the other hand, the entropy generated in each cycle at 2Hz follows a decreasing trend over the fatigue life accompanied by a temperature profile that stabilizes below the glass transition temperature. The lower loading rate allows for the PEKK to undergo larger strains as depicted in Figures 4(c) and (d), hence contributing to a high initial plastic work-induced dissipation. Due to work hardening, the energy generated due to mechanical dissipative phenomena decreases during the material's lifetime which coupled with the low loading frequency allows for the material to exchange energy with the environment. At this stage, thermal equilibrium is attained, and the temperature remains fairly constant until failure.

4.1.3 Thermal Dissipation Entropy

During the fatigue test, heat flows from the specimen to the machine grips by conduction. Using Fourier's law to quantify q_k in equation (5), the evolution of entropy flow due to the heat flux is shown in Figure 6. However, this term can be assumed negligible with respect to the hysteresis entropy since its order of magnitude (10^{-5}) is lower than the hysteresis entropy's (10^{-3}). For this reason, the results obtained above remain unchanged, proving that hysteresis prevails over heat conduction for composites with large temperature gradients.

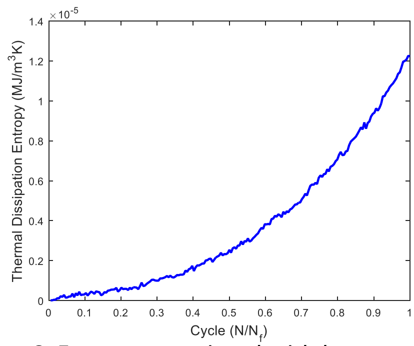

Figure 6. Entropy associated with heat conduction.

4.1.4 Accumulated Entropy

Finally, the accumulated entropy is normalized against the total accumulated entropy at the time of failure and plotted against the normalized fatigue life in Figure 7. The values of γ at failure (i.e., FFE in $\mathrm{MJ/m^3K}$) and fatigue life (N_f) for each loading case are also presented in Table 4.

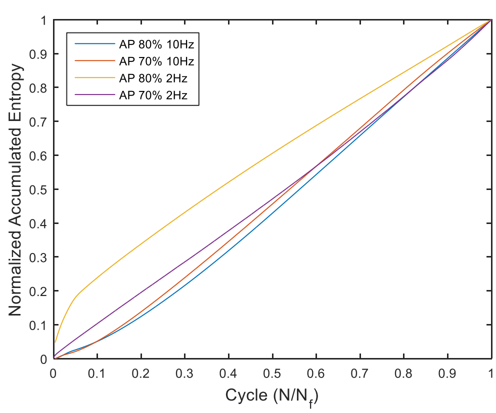

Figure 7. Accumulated entropy.

Table 4. Accumulated entropy at failure and fatigue life.

		2Hz	10Hz
70%	FFE	44.12	0.7321
	N_f	50 332	326
80%	FFE	1.001	0.6023
	N_f	299	214

Unlike most conclusions drawn in related literature, the accumulated entropy at failure due to plastic work for the thermoplastic composite under study is not constant. In addition, the normalized accumulated entropy is also not linearly correlated with the normalized fatigue life, thus compromising the usefulness of entropy as a failure criterion for thermoplastic composites. These discrepancies can be explained by the missing contribution of damage-, viscous- and hardening-related terms to the total generated entropy.

4.2 Quasi-isotropic

4.2.1 Hysteresis Energy

A similar analysis was performed for the quasi-isotropic laminate, with the exception that a small deformation approximation was deemed valid given the small strain amplitude measured with DIC in these tests (i.e., <2% of strain). The hysteresis curves for all the testing conditions are shown in Figure 8.

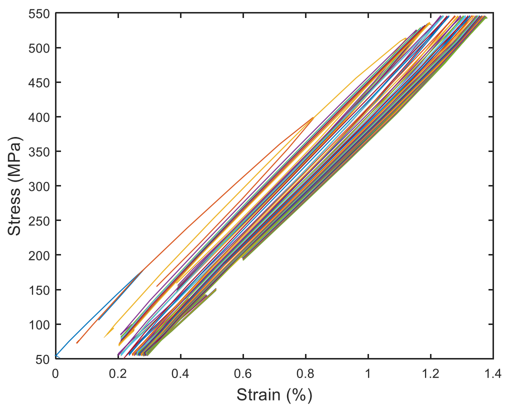

(a) QI_85%_10Hz

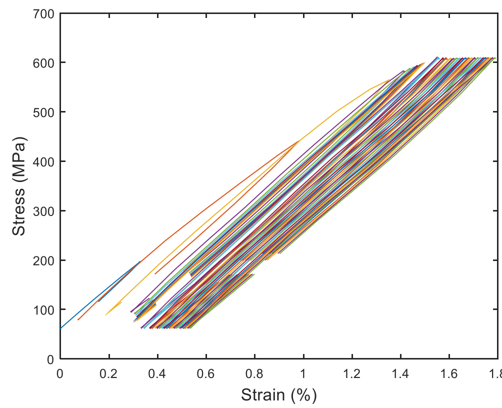

(b) QI_95%_10Hz

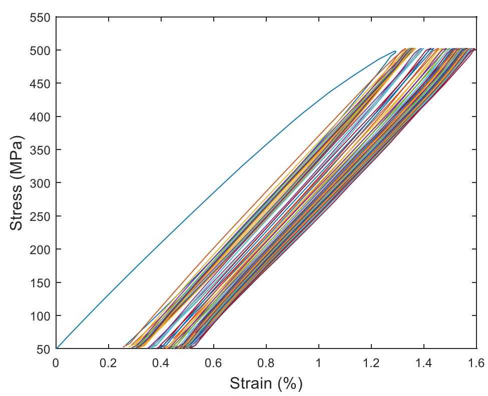

(c) QI_85%_2Hz

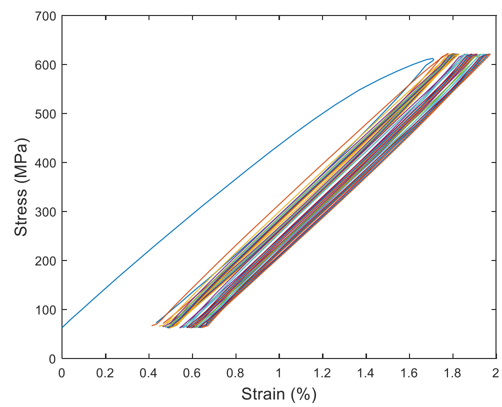

(d) QI_95%_2Hz

Figure 8. Hysteresis loops.

The hysteresis loops are almost overlapping with a small shift in strain throughout the entire test, showing that non-significant irreversible deformation occurs. Also, the areas inside the hysteresis loops are smaller than the angle-ply's, which indicates that most dissipation is originated in the matrix, and it is not as pronounced when fibers are being loaded. Moreover, the higher magnitude of viscoplastic deformation accumulated during the first loading cycles and total strain for the 2Hz cases reveal the rate-dependent behavior of the laminate introduced by some of the off-axis plies in uniaxial loading.

4.2.2 Entropy

Figure 9 represents the evolution of entropy generated per cycle throughout the normalized fatigue life for each of the loading cases. A decreasing trend independent of loading frequency and stress level with a steeper decay within the first 10% of the life can be observed. This initial evolution agrees well with trends of stiffness and temperature evolution in polymer composites where matrix cracking is expected to be more pronounced. Similar to the conclusions drawn from the AP case in section 4.1.4., the accumulated entropy at failure is not constant. However, for this case, an almost linear evolution of entropy generated with the specimen life is observed in Figure 10. The values of FFE (in $\mathrm{MJ/m^3K}$) and fatigue life (N_f) for each loading case are presented in Table 5.

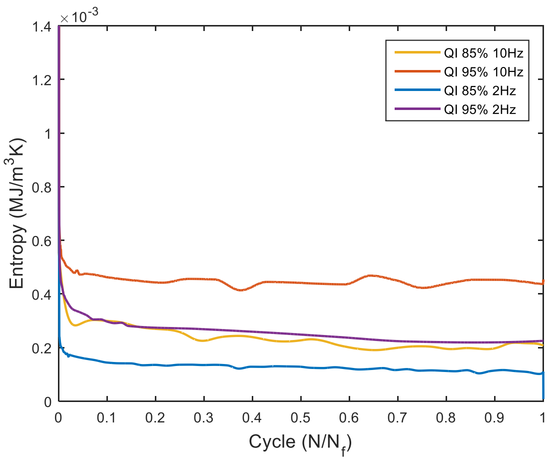

Figure 9. Entropy evolution.

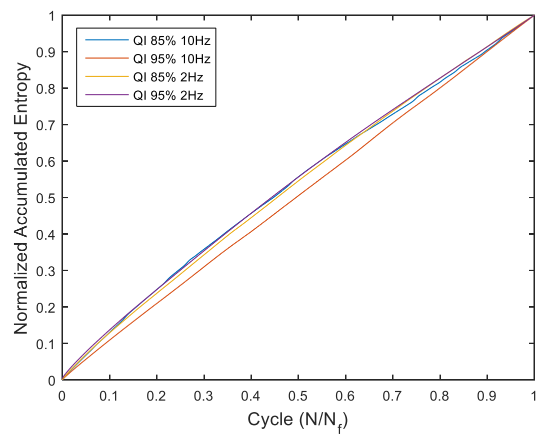

Figure 10. Accumulated entropy.

Table 5. Accumulated entropy at failure and fatigue life.

		2Hz	**10Hz**
85%	**FFE**	5.1719	23.071
	$\mathbf{N_f}$	40 352	91 813
95%	**FFE**	1.7832	8.3820
	$\mathbf{N_f}$	6 968	18 654

The results of FFE for all the loading conditions and stacking sequences were plotted against fatigue life, using a log-log scale in Figure 11. The linear curve fit to the experimental data confirms the power-law dependency of FFE with fatigue life according to the following expression,

$$\text{FFE} = 0.2283 N_f^{0.5908}, \tag{6}$$

with a goodness of $R^2 = 0.55$.

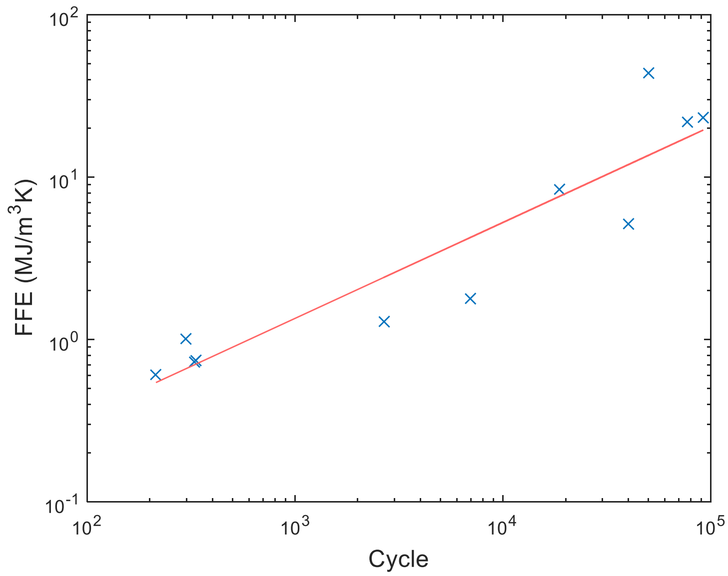

Figure 11. Variation of FFE with the number of cycles to failure.

5 CONCLUSIONS

The entropy generated due to dissipative phenomena during fatigue of PEKK-carbon fiber reinforced composites subjected to different stress and frequency levels was experimentally measured using the hysteresis energy. Contrary to findings reported in the literature, the entropy generated at the time of failure is not constant across all loading conditions and stacking sequences which precludes the widespread implementation of entropy as a failure criterion for thermoplastic composites. Future work will focus on accounting for viscous, damage, and hardening phenomena in the total generated entropy.

6 REFERENCES

[1] P. Irving and C. Soutis (Eds.). "*Polymer composites in the aerospace industry*". 2nd edition, Woodhead Publishing, 2020.

[2] M. Naderi, M. Amiri, and M. Khonsari. "On the thermodynamic entropy of fatigue fracture". *Proceedings of the Royal Society A: Mathematical, Physical and Engineering Sciences*, Vol. 466, No. 2114, pp 423–438, 2010.

[3] M. Naderi and M. Khonsari. "Thermodynamic analysis of fatigue failure in a composite laminate". *Mechanics of Materials*, Vol. 46, pp 113–122, 2012.

[4] B. Mohammadi and A. Mahmoudi. "Developing a new model to predict the fatigue life of cross-ply laminates using coupled CDM-entropy generation approach". *Theoretical and Applied Fracture Mechanics*, Vol. 95, pp 18–27, 2018.

[5] J. Huang, C. Li, and W. Liu. "Investigation of internal friction and fracture fatigue entropy of CFRP laminates with various stacking sequences subjected to fatigue loading". *Thin-Walled Structures*, Vol. 155, No. 106978, 2020.

[6] D. Curtis, D. Moore, B. Slater, and N. Zahlan. "Fatigue testing of multi-angle laminates of CF/PEEK". *Composites Evaluation*, pp 40–50, 1987.